Aerosol and Air Quality Research, 11: 654–663, 2011

ISSN: 1680-8584 print / 2071-1409 online
doi: 10.4209/aaqr.2010.10.0086

Deep Investigation of Ultrafine Particles in Urban Air

Pasquale Avino[1*], Stefano Casciardi[2], Carla Fanizza[1], Maurizio Manigrasso[1]

[1] *DIPIA, INAIL (ex-ISPESL), via Urbana 167, 00184 Rome, Italy*
[2] *DIL, INAIL (ex-ISPESL), via Fontana Candida 1, 00040 Monte Porzio Catone, Italy*

ABSTRACT

This work describes the results of a study which started in 2007 to investigate the ultrafine particle (UFP) pollution in the urban area of Rome. The sampling site was located in a street with high density of autovehicular traffic, where measurements have shown that carbonaceous particulate matter represented an important fraction of aerosol pollution. UFPs have been classified by means of an electrostatic classifier. Monodisperse aerosol was either counted by ultrafine water-based condensation particle counter or sampled by means of a nanometer aerosol sampler. Samples collected were investigated using energy filtered transmission electron microscope in combination with energy dispersive X-ray spectroscopy and electron energy loss spectroscopy. Electron transmission microscope observations revealed that carbonaceous UFPs were present also as nanotube related forms.

The rapid evolution of aerosol from autovehicular exhaust plumes was observed by highly time-resolved aerosol size distribution measurements.

Keywords: Ultrafine particles; Energy Filtered Transmission Electron Microscope analysis; Health effects; Urban air; Carbonaceous aerosol.

INTRODUCTION

Ultrafine particles (UFPs) are recently attracting increasing attention due to their potential effects on human and environmental health (Chen *et al.*, 2010). Their large surface-to-volume ratio and ability to deposit deep in the respiratory tract make UFPs potentially more toxic than their larger counterpart (Nel *et al.*, 2006; Braniš and Větvička, 2010). Several epidemiological studies have shown associations between ambient ultrafine particles and adverse respiratory and cardiovascular effects (Peters *et al.*, 1997), resulting in morbidity and mortality in susceptible subpopulations. A high deposition efficiency of UFPs in the pulmonary region was demonstrated in healthy subjects (Brown *et al.*, 2002) and an increased deposition was observed in patients with asthma (Chalupa *et al.*, 2004) or chronic obstructive lung diseases (Brown *et al.*, 2002). The mechanisms for the cardiovascular effects are not completely understood, but a possible hypothesis is that, because of their small size, UFPs could enter the systemic circulation and induce direct effects on myocardium or coronary vasculature (Nemmar *et al.*, 2004). Several studies have indicated that about 50–70% of UFP mass consists of carbonaceous material (Puxbaum and Wopenka, 1984; Berner *et al.*, 1996; Hughes *et al.*, 1998; Chen *et al.*, 2010; Zhu *et al.*, 2010b). Combustion-derived ultrafine particles, such as diesel soot, are the most numerous particles, by number, in urban PM_{10}. Carbon particle aggregates containing substances like Fe, other transition metals, Volatile Organic Compounds (VOCs) and polycyclic aromatic hydrocarbons, have been associated with the inflammatory reaction caused by particles (Gilmour *et al.*, 1996; Johnston *et al.*, 1996; Osier and Oberdorster, 1997; Vedal, 1997; Venkataraman and Raymond, 1998).

The carbonaceous material (total carbon, TC) is classified into elemental carbon (EC) or black carbon (BC), depending on thermal or optical properties respectively (Cachier *et al.*, 1989; Zhu *et al.*, 2010a), and organic carbon (OC). The EC fraction has a graphitic structure: it is a primary pollutant emitted directly during combustion processes (Avino *et al.*, 2000; Zhu *et al.*, 2010a; Zhu *et al.*, 2010b). The OC fraction is composed by different classes of compounds (hydrocarbons, oxygenated compounds, etc.): it has both primary and secondary origins. The primary OC (OC_{prim}) is emitted as sub-micron particles or from biogenic plant emission, whereas the secondary OC (OC_{sec}) may originate from gas-particle condensation of VOCs with low vapour pressure, by chemical-physical adsorption of gaseous species on particles or as product from photochemical atmospheric reactions (Mohler *et al.*,

* Corresponding author. Tel: 39-06-9789-3036;
Fax: 39-06-9789-3004
E-mail address: pasquale.avino@ispesl.it

1997). TC particles act as carriers of toxic compounds inside the human respiratory system causing Chronic Obstructive Respiratory Diseases (CORDs) and/or new pathologies related with the pollutants delivered (Avino *et al.*, 2004). In recent years several worldwide studies on aerosol particle number concentrations and size distribution have been published (Hussein *et al.*, 2003; Buonanno *et al.*, 2009; Buonanno *et al.*, 2010; Chen *et al.*, 2010; Liu *et al.*, 2010; Zhu *et al.*, 2010b). Because of lack of relevant data in the urban area of Rome, a study has been undertaken on UFP number size distribution and composition, starting from measuring carbonaceous particulate matter. UFPs were investigated by Scanning Mobility Particle Sizer (SMPS) and Fast Mobility Particle Sizer (FMPS) analyzers and were collected by a Nanometer Aerosol Sampler (NAS) and observed by EFTEM.

METHODS

Site Description

Aerosol and gas-phase pollutant (CO and NO_x) measurements were carried out at the Pilot Station located in a street canyon in downtown Rome at the ISPESL's building (near S. Maggiore Cathedral). The site is characterized by high density of autovehicular traffic. Carbonaceous aerosol measurements were performed in the green park of Villa Ada as well, where samples for the chemical characterization of OC were also taken. Seasonal measurements of OC and EC and UFP number size distribution were carried out from 2007 at ground level.

PM_{10} and Carbonaceous Aerosol Measurements

PM_{10} measurements were performed with a Tapered Element Oscillating Microbalance (TEOM) Ambient Particulate monitor (Rupprecht & Patashnik Co Inc., Albany, NY, USA).

The EC and OC separation was carried out by means of an Ambient Carbon Particulate Monitor 5400 (ACPM 5400, Rupprecht & Patashnik Co Inc.) equipped with a 10 μm-sampling head. The ACPM 5400 is based on a two-step combustion procedure. By means a non-dispersive infrared detector (NDIR) the instrument measures the CO_2 amount released when a particulate matter sample collected in a collector is oxidized at elevated temperatures. The instrument measures the OC concentration at 350°C and the TC concentration at the 750°C. EC is calculated as difference of TC and OC. Aerosol samples for the chemical characterization of OC were collected on glass fiber filters by means of a high volume aspirating pump equipped with a 10 μm sampling head. Each sampling lasted 12 or 24 h. The method of extraction and analysis was described in detail in a previous publication (Marino *et al.*, 2002). The OC_{sec} fraction was assessed using EC as a tracer of OC_{pri} (Castro *et al.*, 1999) by the equation:

$$OC_{\sec} = OC_{total} - \left(\frac{OC}{EC}\right)_{\min imum} \times EC \quad (1)$$

The calculation relies on the estimate of the primary OC/EC ratio that is assumed to be associated to samples with minimum OC/EC values, OC/EC ratios greater than $(OC/EC)_{min}$ indicate that secondary OC formation occurred.

Gas-phase Pollutants

Carbon monoxide and NO_x concentrations have been measured by means of a Recordum Airpointer analyzer (Airpointer, Mödling, Austria).

UFP Number-size Distribution Measurements

Aerosol number size distributions were measured using a Scanning Mobility Particle Sizer (SMPS, model 3936, TSI, Shoreview, MN USA) equipped with an Electrostatic Classifier (model 3080, TSI) and a Differential Mobility Analyzer (DMA, model 3085, TSI), for the electrical mobility diameter size classification of the particles. The charge equilibrium for the sample flow was obtained by a bipolar ^{85}Kr aerosol neutralizer (model 3077, TSI) before entering the DMA (Wiedensohler, 1988). At the exit of DMA particles were either counted with a water-based Condensation Particle Counter (model 3786, TSI), or sampled by means of a nanometer aerosol sampler (model 3089, TSI). The aerosol and the sheath air volume flow rates of the DMA were equal to 0.5 and 5 L/min, to measure particle number concentration over the size range 3.5 to 117 nm electrical mobility diameter. The time resolution for the whole size range was 5 min.

Highly time-resolved particle number size distributions (1 s time) were measured by means of a Fast Mobility Particle Sizer (FMPS, model 3091, TSI) in the range from 5.6 to 560 nm electrical mobility diameter.

Sampling and TEM Sample Preparation

The nanometer aerosol sampler (TSI 3089) consists of grounded cylindrical sampling chamber with an electrode at its bottom. The sampler operated at 0.75 L/min, and –7 keV. Particles were collected due to the electric field applied between the chamber and the electrode. Samples were collected over 12 h sampling time. Particles on TEM grids (standard 300-mesh copper grids coated with carbon film) were investigated using Energy Filtered Transmission Electron Microscope (EFTEM). Conventional and high resolution TEM micrographs were acquired to get morphological information. The elemental analysis was carried out by means of energy dispersive X-ray spectroscopy (EDS). TEM experiments were performed by a FEI TECNAI 12 G2 Twin operated at an accelerating voltage of 120 kV, equipped with an electron energy filter (Gatan Image Filter, BioFilter model) and a Peltier cooled charge-coupled device based slow scan camera (Gatan multiscan camera, model 794).

RESULTS AND DISCUSSION

Carbonaceous Aerosol Measurements

The carbonaceous material represents an important contribution to the aerosol pollution in downtown Rome, as shown in Fig. 1 reporting the cumulative frequency distribution of the percent contribution of TC to PM_{10} in

winter and summer seasons. In both seasons most frequent TC data are between 20% and 40 % of PM_{10}. Higher TC/PM_{10} ratios (40–60%) are relatively more frequent in summer than in winter due to the greater photochemical contribution. The OC contribution to the carbonaceous PM in winter and summer is described in Fig. 2. The OC percentage varies depending on the season and the sampling point. In fact, in downtown Rome, where the pollution sources are dominated by anthropogenic emissions, OC/TC is between 25–60% with a mean value around 42% in cold period and between 30–65% with a mean of 47% during hot period. The situation is quite different inside the green park "villa Ada" where the anthropogenic emissions do not affect directly the OC/TC levels (0.52 and 0.59 in cold and hot period, respectively): villa Ada park is considered as representative of Rome background pollution. The OC and EC levels were similar to the literature values found in different cities at ground level (Table 1). The

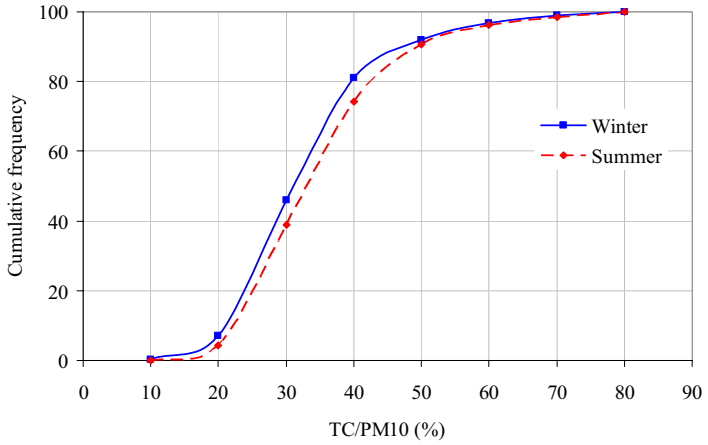

Fig. 1. Cumulative frequency distribution of the % contribution of TC to PM_{10} in summer and winter seasons in downtown Rome.

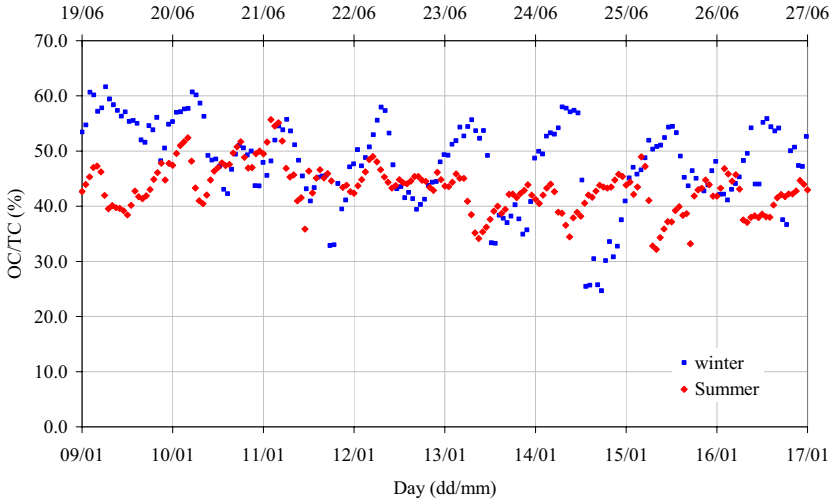

Fig. 2. OC/TC ratios in summer and winter seasons in downtown Rome.

Table 1. Values (μg/m^3) of atmospheric carbonaceous particulate in various urban areas.

Environment	Location	TC	EC	OC	OC/TC	Reference
Urban	Nagoya–Japan	13–65	5–34	7–34	0.56	Kadowaki (1990)
Urban	26 cities–U.S.A.	10.3	3.8	6.6	0.64	Shah *et al.* (1982)
Urban	Toronto–Canada	6.44	2–12	–	–	Pimenta and Wood (1980)
Urban	Athens–Greece	7.1–13.7	2.1-5.5	4.9–8.3	0.6–0.7	Prosmitis *et al.* (2004)
Urban	Paris–France	21.0	4.6	16.4	0.78	Bremond *et al.* (1989)
Suburban	Gif sur Yvette–France	9.7	2.2	7.5	0.77	Bremond *et al.* (1989)
Remote	Ivory Coast	10.1	1.5	8.6	0.85	Cachier *et al.* (1989)
Urban	Rome–Italy	14–23	8–12	6–11	0.45	
Park	Rome Villa Ada	7–12	3-5	4–7	0.57	

percent contribution of OC_{sec} to OC was 36% in summer and 29% in winter. These results are coherent with the radical oxidative activity expected higher in summer than in winter. The compounds identified in the OC fraction which may have an important effect on human health are Polycyclic Aromatic Hydrocarbons (PAHs), n-alkanes and n-alkanoic acids. Typical average concentrations are reported in Table 2.

UFP Number-size Distributions

Total UFP number concentrations showed a typical daily modulation with peak values during periods of maximum autovehicular traffic intensity and of solar radiation. Minimum values were measured during nocturnal hours, when the effect due to the reduction of the autovehicular traffic emission overcomes the decrease of the atmospheric mixing height. Daily trends of hourly-average UFP number concentrations were substantially similar during the periods investigated (Fig. 3) with daily averages ranging from 23,100 to 42,000 1/cm^3 and from 13,400 to 45,000 1/cm^3, respectively in April–May 2008 and in January 2009.

Figs. 4(a) and 4(b) show the scatter plots of UFP number concentrations, in the ranges 3–10 nm and 50–117 nm, and nitrogen oxides, in April–May 2008 and January 2009, respectively. The range 3–10 nm, includes particles in the nucleation mode formed directly from the gas/vapour phase, whereas the range 50–117 nm refers to particles in the Aitken mode, that have aged and grown somewhat.

While for the particles in the range 50–117 nm the correlation with nitrogen oxides is pretty good with a Pearson correlation coefficient of 0.7 in both periods, the particles in the nucleation mode are basically uncorrelated (Pearson correlation coefficient of 0.1 and 0.3 respectively in May–April 2008 and January 2009). This can be explained considering that such kind of particles are not only freshly emitted by combustion sources but are also formed by homogeneous nucleation in atmosphere: in this case they depends both on the degree of atmospheric radical activity and on the dilution conditions of engine exhausts. Confirming the main origin due to autovehicular traffic, UFP number concentrations (hourly averages) displayed similar patterns of variation as carbon monoxide (hourly averages), a typical primary pollutant associated to the autovehicular exhaust (Fig. 5(a)). Differences in the trends of the two pollutants were, however, observed, as shown in Fig. 5(b), when UFP trend displayed a peak with maximum value between 12 am and 1 pm. In the same period, CO concentration profile was fairly constant, implying that the peak observed for UFPs did not arise directly from primary autovehicular emissions.

Although highly size-resolved measurements, SMPS data are not the most appropriate to study fast evolution of aerosols such as those related to engine exhausts, due to the relatively high response time. Particle formation episodes, occurring in the time scale of few seconds, were detected with FMPS measurements. An example is reported in Fig. 6, describing the particle size distribution in the range 5.6–560 nm as a function of time and showing an abrupt increase of particle number concentration. Such

Table 2. Average concentrations (ng/m^3) of *n*-alkanes, *n*-alkanoic acids and PAHs measured in villa Ada Park.

n-alkane	
n-Heptadecane	16.3
n-Octadecane	18.2
n-Nonadecane	14.7
n-Eicosane	12.0
n-Heneicosane	12.7
n-Docosane	15.5
n-Tricosane	14.8
n-Tetracosane	11.0
n-Pentacosane	6.2
n-Hexacosane	4.3
n-Heptacosane	4.3
n-Octacosane	2.2
n-Nonacosane	3.2
n-Triacontane	1.2
n-Hentriacontane	2.1
n-Dotriacontane	0.6
n-Tritriacontane	0.7
n-Tetratriacontane	0.1
Total *n*-alkanes (C17–C34)	**140.1**
n-Alkanoic acid	
n-Dodecanoic acid	2.5
n-Tridecanoic acid	0.3
n-Tetradecanoic acid	4.5
n-Pentadecanoic acid	2.4
n-Hexadecanoic acid	14.0
n-Heptadecanoic acid	0.9
n-Octadecanoic acid	4.5
n-Nonadecanoic acid	0.1
n-Eicosanoic acid	0.4
n-Heneicosanoic acid	0.1
n-Docosanoic acid	0.2
n-Tricosanoic acid	0.1
n-Tetracosanoic acid	0.5
n-Pentacosanoic acid	0.1
n-Hexacosanoic acid	0.1
n-Heptacosanoic acid	0.0
n-Octacosanoic acid	0.1
Total *n*-akanoic acid (C12–C28)	**30.8**
Polyciclic Aromatic Hydrocarbons	
Fenantrene	1.5
Fluoranthene	3.6
Pyrene	3.7
Benz(a)anthracene	2.5
Chrysene	3.8
Benzo(b)fluoranthene	2.7
Benzo(k)fluoranthene	0.7
Benzo(e)pyrene	1.2
Benzo(a)pyrene	1.3
Indenopyrene	0.5
Dibenzo(ah)anthracene	0.1
Benzo(ghi)perylene	0.8
Total PAHs	**22.4**

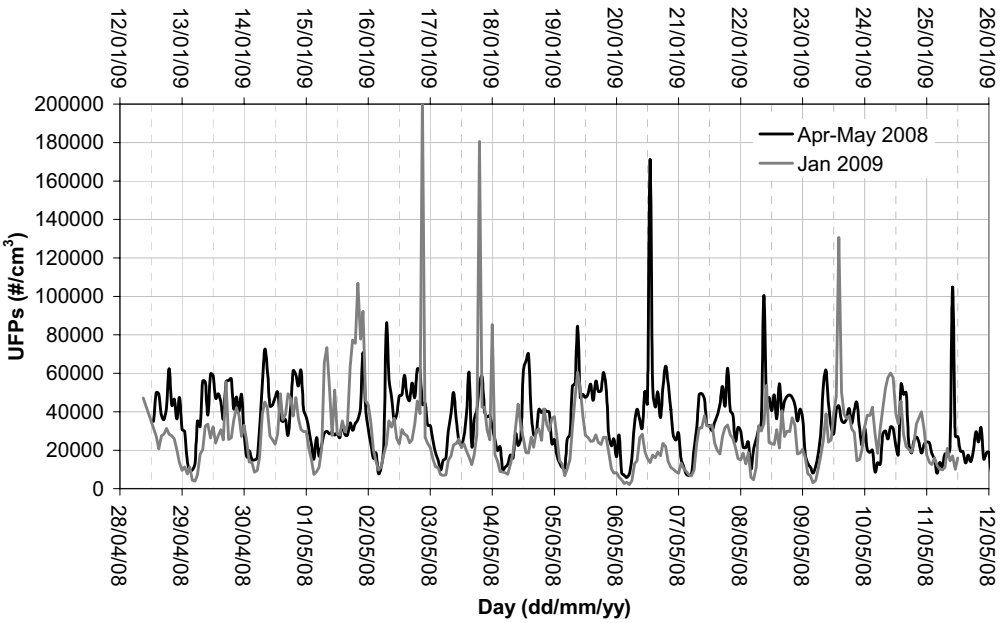

Fig. 3. Daily trends of total UFP number concentrations in April–May 2008 and January 2009.

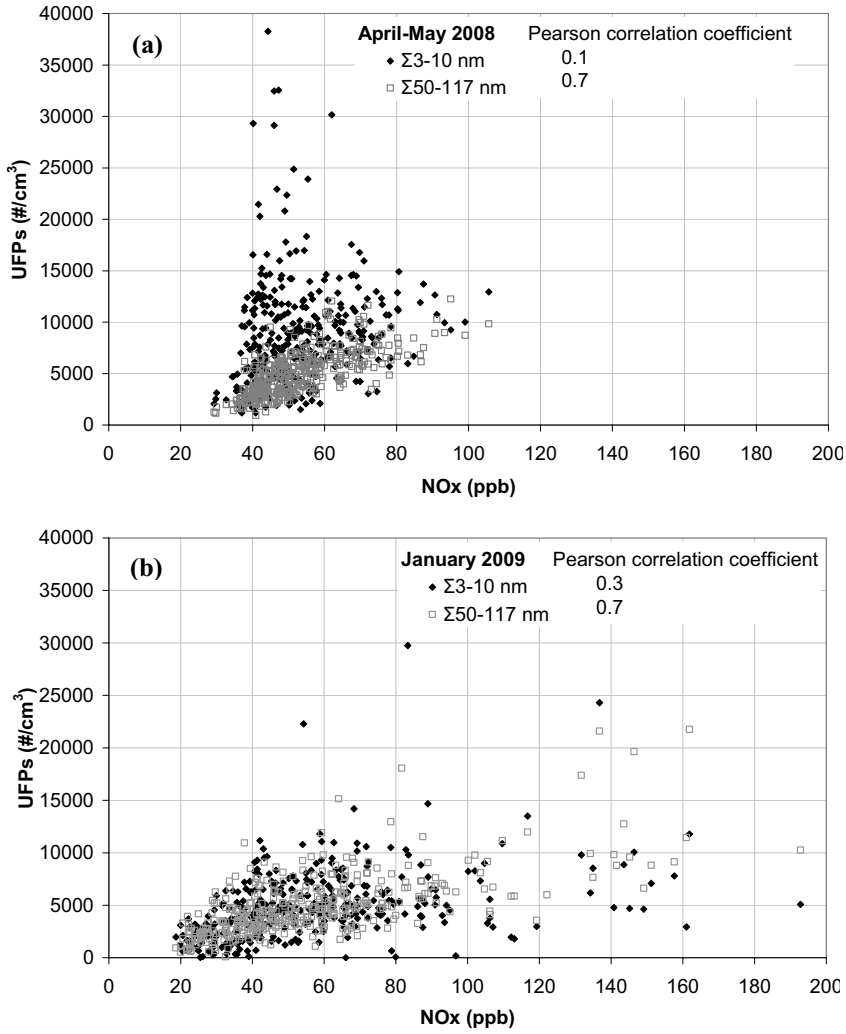

Fig. 4. Scatter plots of nitrogen oxides and UFPs in the ranges 3–10 nm and 50–117 nm in April–May 2008 (a) and in January 2009 (b).

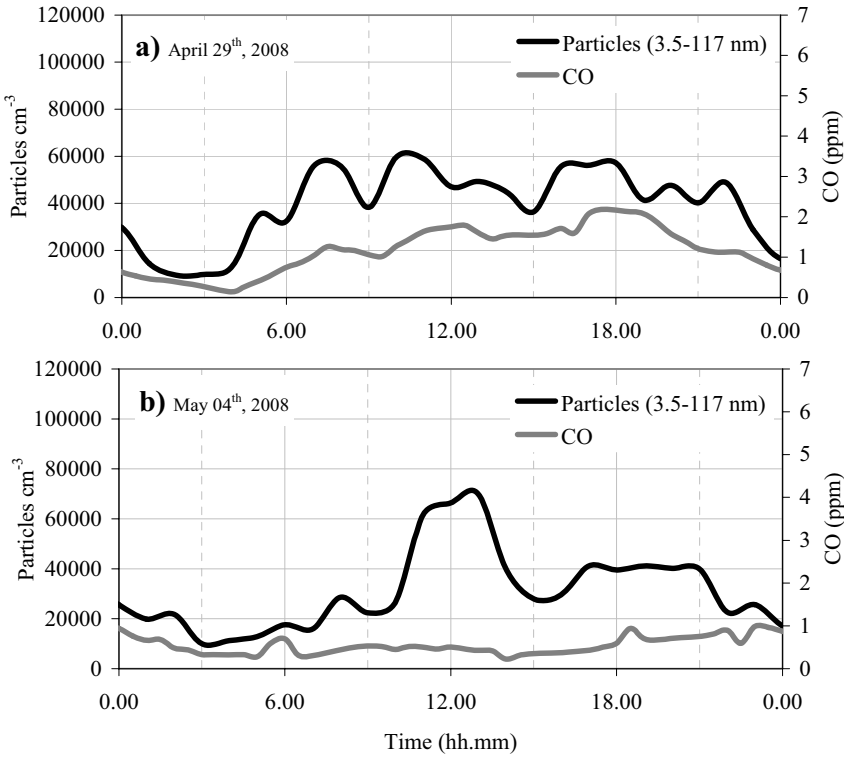

Fig. 5. UFP number and carbon monoxide concentrations. Examples of common (a) and different (b) trends of variation.

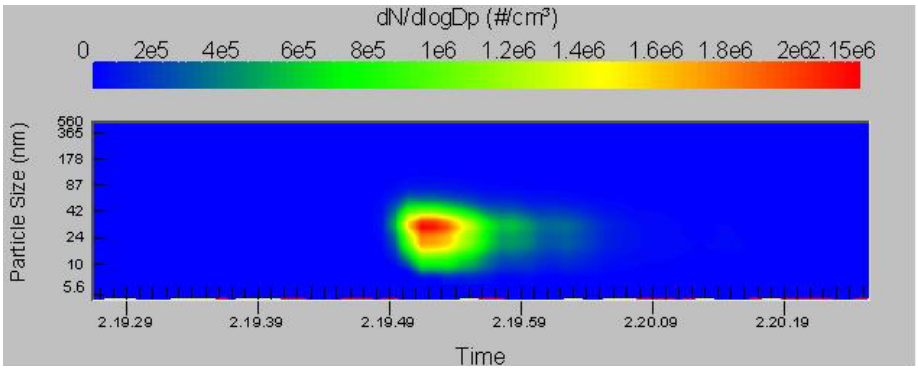

Fig. 6. Nocturnal particle formation episode in the time scale of 10 s detected with FMPS.

episode, clearly not ascribable to a photochemical induced mechanism, since occurring during nocturnal hours, was probably due to particle nucleation from supersaturated vapour in a combustion exhaust plume. Within few seconds particle number size distributions changed with about a hundred-fold increase of concentration of particles in the nucleation mode (Figs. 7(a) and 7(b)). Favoured by the lower nocturnal temperatures and by the lower levels of total particle number concentration, implying less surface available for the competing condensation of supersaturated gaseous species, peak values of total particle number concentration by far exceed the values measured during diurnal rush hours (Fig. 8).

Transmission Electron Microscope Analysis

Mobility-classified ultrafine particles were distinguished based on morphological and chemical information obtained with the EFTEM-EDS. 76% of the particles analyzed were composed of carbon (Fig. 9(a)), they presented oval, spherical or polyhedrical shape.

Carbonaceous nanocrystal aggregates were collected, containing also carbon nanotubes. An example is shown in Fig. 9(b), where the inset displays a detail of the nanotube edges obtained by a High Resolution TEM micrograph. Fullerenes and carbon nanotubes occur naturally and have been found in hydrocarbon flames (acetylene, benzene, ethylene) and natural gas (96% methane)/air and propane/air combustion exhausts (Murr *et al.*, 2004). Moreover, carbon nanotubes were observed in a small fraction of soot collected by thermophoretic precipitation from wood burning in air (Murr and Guerrero, 2006).

12.8% of the particles were constituted mainly of carbon with traces of other elements such as K, Mg, Si and N. Moreover, 6.3% of the particles included: elongated

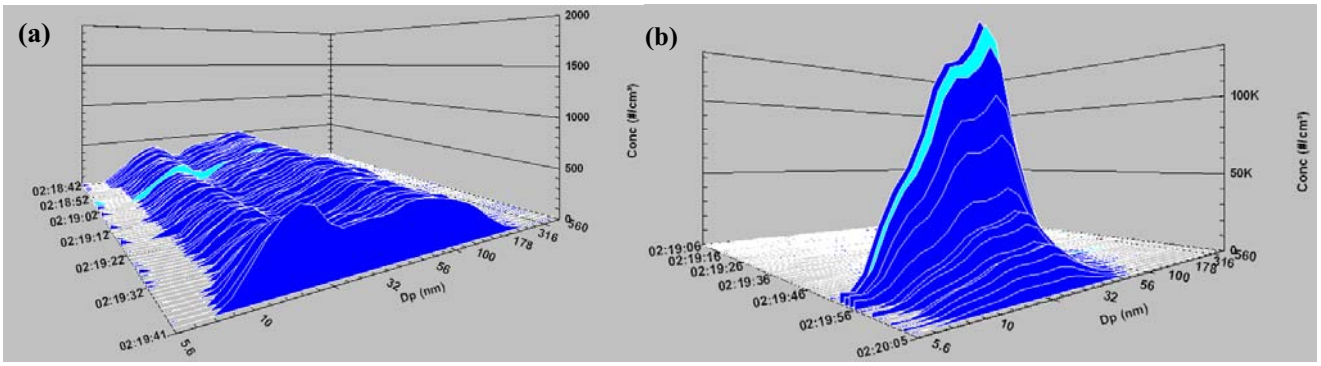

Fig. 7. Highly time-resolved evolution of the aerosol number size distribution: soon before (a) and during (b) the episode described in Fig. 6.

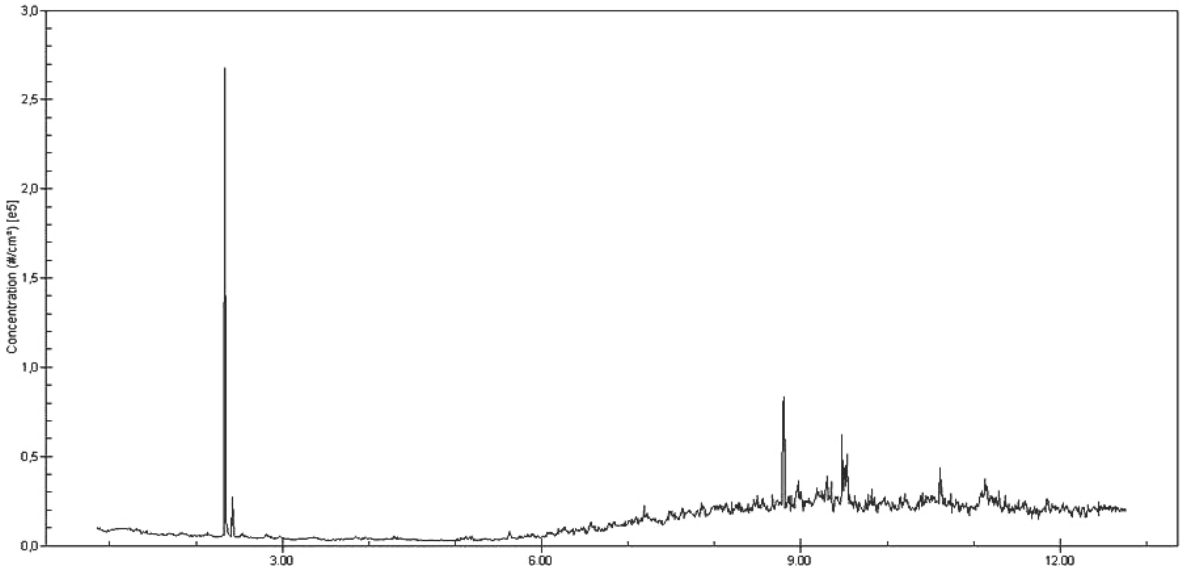

Fig. 8. 30 s-averaged total (5.6–620 nm) particle number concentration referring to the episode described in Fig. 6.

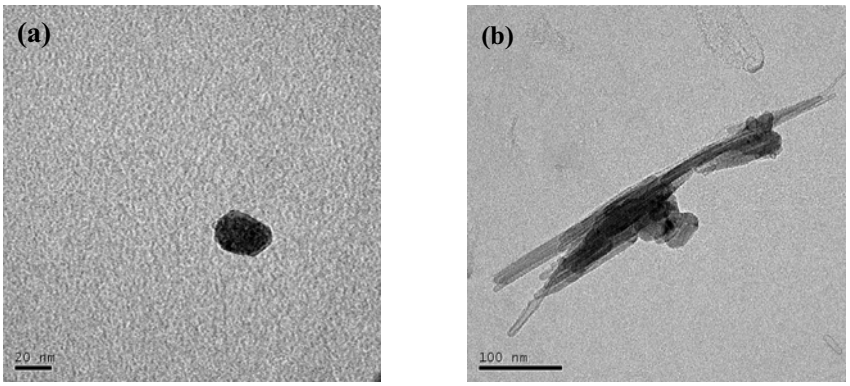

Fig. 9. TEM micrographs of carbonaceous particle (a) and carbon nanotube aggregate (b).

particles containing Mg, Fe; particles constituted by Mg, Cr, Fe, Ni and particles composed of Fe, Ni. An example of particle constituted by Fe and Ni is reported in Fig. 10(a) showing a bright field (BF) micrograph obtained by Scanning Transmission Electron Microscope (STEM). Fig. 10(b) shows the EDS spectrum acquired at the point corresponding to the circle reported in the STEM micrograph. All EDS spectra exhibit high Cu peaks that originate from the Cu grids and the sample holder. 1.8% of particles consisting mostly of Si were also detected.

Studies conducted in different sites of California detected the presence of trace metal concentrations in UFPs. The most abundant catalytic metals measured in the ultrafine particles, in the atmosphere of seven cities in

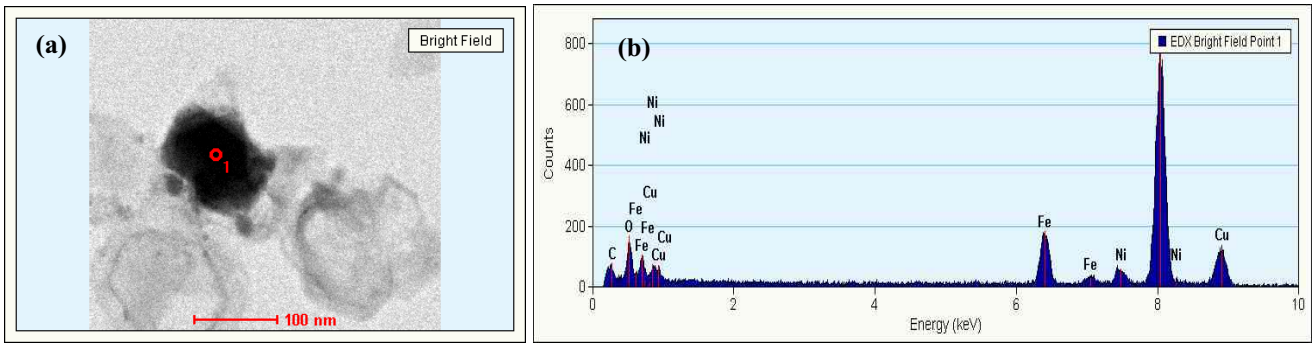

Fig. 10. STEM BF micrograph of nickel and iron particle (a) and relative EDS spectrum (b).

Southern California, were Fe, Ti, Cr, Zn (Cass *et al.*, 2000). The same transition metals were found at Pasadena (Hughes *et al.*, 1998), while Fe, Cu and Zn were detected in the ultrafine size range at Bakersfield, CA (Chung *et al.*, 2001). A study conducted in two urban areas of Southern California, Downey and Riverside, found that Fe was the most abundant transition metal in both locations followed by Cu, Zn, Cr, V and Ni (Kim *et al.*, 2002). Moreover, a study on the chemical properties of ultrafine particles in the Helsinki area showed metal concentrations in the Aitken mode (Pakkanen *et al.*, 2001): the presence of Mg, Ca, Sr was attributed to vehicle exhausts and Fe, Co, Ni, Mo to heavy fuel oil combustion.

CONCLUSIONS

Seasonal measurements of OC and EC showed that the carbonaceous fraction in downtown Rome accounted for 20–40% of the PM_{10} at ground level. In downtown Rome the OC average contribution to TC was about 47% and 42%, in summer and winter seasons respectively. In the background area of villa Ada OC represented 59% of TC in summer and 52% in winter. The presence of n-alkanes (total level 140.1 ng/m^3), n-alkanoic acids (total level 30.8 ng/m^3) and PAHs (total level 22.4 ng/m^3) in PM composition should be underlined.

Total UFP concentration followed a daily trend governed by both the evolution of the atmospheric mixing height and the variation of the autovehicular traffic intensity. The good correlation of particle number concentration in the range 50–117 nm and nitrogen oxides confirmed the role played by the autovehicular traffic as the main source of UFPs. The lack of correlation between particles in the nucleation mode and nitrogen oxides evidenced the important contribution due to the formation of new particles from the gas phase. Such contribution occurs through radical photooxidative processes or through condensation of supersaturated vapours from autovehicular exhausts, as evidenced by highly time-resolved aerosol size distribution measurements. The differences observed in the trends of variation of UFPs and carbon monoxide confirmed such findings. The role of photochemical processes was also confirmed by the higher contribution of OC_{sec} to OC estimated in summer than in winter.

Moreover, EFTEM equipped with EDS was employed for morphological and chemical characterization of mobility-classified ultrafine particles. TEM analyses, evidencing the presence of nanotube related forms and transition metals in the ultrafine size range, have shown the need for further studies on the structure, morphology and chemical composition of UFPs.

The integrated approach of aerosol size distribution measurements and TEM characterization can furnish useful information to toxicologists regarding both the size related deposition efficiency of particles in the respiratory tract and their biological activity linked to the chemical composition.

ACKNOWLEDGMENTS

This work was supported under the grant ISPESL/DIPIA/P6 “Identificazione, analisi e valutazione delle conseguenze delle attività antropiche” L4, L5, L6, the PMS/40/06/P8 grant of the Ministry of the Health, and ISPESL/DIL/P6 “Metodologie di analisi per la caratterizzazione di materiale particellare fibroso” L3.

The authors wish to thank the two anonymous reviewers for the improvement of the manuscript quality through their valuable revisions.

REFERENCES

Avino, P., Brocco, D., Lepore, L. and Ventrone, I. (2000). Distribution of Elemental Carbon (EC) and Organic Carbon (OC) in the Atmospheric Aerosol Particles of Rome. *J. Aerosol Sci.* 31: S364–S365.

Avino, P., De Lisio, V., Grassi, M., Lucchetta, M.C., Messina, B., Monaco, G., Petraccia, L., Quartieri, G., Rosentzwig, R., Russo, M.V., Spada, S. and Valenzi, V.I. (2004). Influence of Air Pollution on Chronic Obstructive Respiratory Diseases: Comparison between City (Rome) and Hillcountry Environments and Climates. *Ann. Chim. (Rome)* 94: 629–636.

Berner, A., Sidla, S., Galambos, Z., Kruisz, C., Hitzenberger, R., Ten Brink, H.M. and Kos, G.P.A. (1996). Modal Character of Atmospheric Black Carbon Size Distributions. *J. Geophys. Res.* 101: 19559–19565.

Braniš, M. and Větvička, J. (2010). PM_{10}, Ambient Temperature and Relative Humidity during the XXIX Summer Olympic Games in Beijing: Were the Athletes at Risk? *Aerosol Air Qual. Res.* 10: 102–110.

Bremond, M.P., Cachier, H. and Buat-Méenard, P. (1989). Particulate Carbon in the Paris Region Atmosphere. *Environ. Technol.* 10: 339–346.

Brown, J.S., Zeman, K.L. and Bennett, W.D. (2002). Ultrafine Particle Deposition and Clearance in the Healthy and Obstructed Lung. *Am. J. Respir. Crit. Care Med.* 166: 1240–1247.

Buonanno, G., Ficco, G. and Stabile, L. (2009). Size Distribution and Number Concentration of Particles at the Stack of a Municipal Waste Incinerator. *Waste Manage.* 29: 749–755.

Buonanno, G., Anastasi, P., Di Iorio, F. and Viola, A. (2010). Ultrafine Particle Apportionment and Exposure Assessment in Respect of Linear and Point Sources. *Atmos. Pollut. Res.* 1: 36–43.

Cachier, H., Bremond, M.P. and Buat-Ménard, P. (1989) Determination of Atmospheric Soot Carbon with a Simple Thermal Method. *Tellus B* 41: 379–390.

Cass, G.R., Hughes, L.A., Bhave, P., Kleeman, M.J., Allen, J.O. and Salmon, L.G. (2000). The Chemical Composition of Atmospheric Ultrafine Particles. *Philos. Trans. R. Soc. London, Ser. A* 358: 2581–2592.

Castro, L.M., Pio, C.A., Harrison, R.M. and Smith D.J.T. (1999). Carbonaceous Aerosol in Urban and Rural European Atmospheres: Estimation of Secondary Organic Carbon Concentrations. *Atmos. Environ.* 33: 2771–2781.

Chalupa, D.C., Morrow, P.E., Oberdörster, G., Utell, M.J. and Frampton, M.W. (2004). Ultrafine Particle Deposition in Subjects with Asthma. *Environ. Health Perspect.* 112: 879–882.

Chen, S.C., Tsai, C.J., Huang, C.Y., Chen, H.D., Chen, S.J., Lin, C.C., Tsai, J.H., Chou, C.C.K., Lung, S.C.C., Huang, W.R., Roam, G.D., Wu, W.Y., Smolik, J. and Dzumbova, L. (2010). Chemical Mass Closure and Chemical Characteristics of Ambient Ultrafine Particles and other PM Fractions. *Aerosol Sci. Technol.* 44: 713–723.

Chung, A., Herner, J.D. and Kleeman, M.J. (2001). Detection of Alkaline Ultrafine Atmospheric Particles at Bakersfield, California. *Environ. Sci. Technol.* 35: 2184–2190

Gilmour, P.S., Brown, D.M., Lindsay, T.G., Beswick, P.H., MacNee, W. and Donaldson, K. (1996). Adverse Health Effects of PM_{10} Particles: Involvement of Iron in Generation of Hydroxyl Radical. *Occup. Environ. Med.* 53: 817–822.

Hughes, L.S., Cass, G.R., Gone, J., Ames, M. and Olmez, I. (1998). Physical and Chemical Characterization of Atmospheric Ultrafine Particles in the Los Angeles area. *Environ. Sci. Technol.* 32: 1153–1161

Hussein, T., Puustinen, A., Aalto, P.P., Makela, J.M., Hameri, K. and Kulmala, M. (2003). Urban Aerosol Number Size Distributions. *Atmos. Chem. Phys. Discuss.* 3: 5139–5184.

Johnston, C.J., Finkelstein, J.N., Gelein, R., Baggs, R. and Oberdorster, G. (1996). Characterization of the Early Pulmonary Inflammatory Response Associated with PTFE Fume Exposure. *Toxicol. Appl. Pharmacol.* 140: 154–163.

Kadowaki, S. (1990). Characterization of Carbonaceous Aerosols in the Nagoya Urban Area. 1. Elemental and Organic Concentrations and the Origin of Organic Aerosols. *Environ. Sci. Technol.* 24: 741–744.

Kim, S., Shen, S., Sioutas, C., Zhu, Y. and Hinds, W.C. (2002). Size Distribution and Diurnal and Seasonal Trends of Ultrafine Particles in Source and Receptor Sites of the Los Angeles Basin. *J. Air Waste Manage. Assoc.* 52: 297–307.

Liu, B.Y.H., Romay, F.J., Dick, W.D., Woo, K.S. and Chiruta, M. (2010). A Wide-range Particle Spectrometer for Aerosol Measurement from 0.010 μm to 10 μm. *Aerosol Air Qual. Res.* 10: 125–139.

Marino, F., Cecinato, A. and Siskos, P.A. (2000). Nitro-PAH in Ambient Particulate Matter in the Atmosphere of Athens. *Chemosphere* 41: 533–537.

Mohler, O., Naumann, K.H, Saathoff, F. and Schurath, U. (1997). The Influence of Soot Surface Reaction on the Ozone and NO_x Chemistry. *J. Aerosol Sci.* 28: S309–S310.

Murr, L.E., Bang, J.J, Esquivel, E.V., Guerrero, P.A. and Lopez, D.A. (2004). Carbon Nanotubes, Nanocrystal Forms, and Complex Nanoparticle Aggregates in Common Fuel-gas Combustion Sources and the Ambient Air. *J. Nanopart. Res.* 6: 241–251.

Murr, L.E. and Guerrero, P.A. (2006). Carbon Nanotubes in Wood Soot. *Atmos. Sci. Lett.* 7: 93–95

Nel, A., Xia, T., Mädler, L. and Li, N. (2006). Toxic Potential of Materials at the Nanolevel. *Science* 311: 622–627.

Nemmar, A., Hoylaerts, M. F., Hoet, P. H. M. and Nemery, B. (2004). Possible Mechanisms of the Cardiovascular Effects of Inhaled Particles: Systemic Translocation and Prothrombotic Effects. *Toxicol. Lett.* 149: 2443–2253.

Osier, M. and Oberdorster, G. (1997). Intratracheal Inhalation vs. Intratracheal Instillation: Differences in Particle Effects. *Fundam. Appl. Toxicol.* 40: 220–227.

Pakkanen, T.A., Kerminen, V.M., Korhonen, C.H., Hillamo, R.E., Aarnio, P., Koskentalo, T. and Maenhaut, W. (2001). Urban and Rural Ultrafine ($PM_{0.1}$) Particles in the Helsinki Area. *Atmos. Environ.* 35: 4593–4607.

Peters, A., Doring, A., Wichmann, H.E. and Koenig, W. (1997). Increased Plasma Viscosity during an Air Pollution Episode: A Link to Mortality? *Lancet* 349: 1582–1587.

Pimenta, J. and Wood, G.R. (1980). Determination of Free and Total Carbon in Suspended Air Particulate Matter Collected on Glass Fiber Filters. *Environ. Sci. Technol.* 14: 556–561.

Prosmitis, A.B., Diapouli, E., Grivas, G., Chaloulakou, A. and Spyrellis, N. (2004). Continuous Field Measurements of Organic and Elemental Carbon Concentrations in Athens, Greece. *J. Aerosol Sci.* 35: S1077–S1078.

Puxbaum, H. and Wopenka, B. (1984). Chemical Composition of Nucleation and Accumulation Mode Particles Collected in Vienna, Austria. *Atmos. Environ.* 18:573–580.

Shah, J.J., Johnson, R.L., Heyederdahl, E.K. and Huntzicker, J.J. (Ed.) Carbonaceous Aerosol at Urban and Rural Sites in the United States, Proc. 75th Ann. Meet. Air Poll.

Control Ass., New Orleans, 1982, Lousiana, p. 20–25.

Vedal, S. (1997). Ambient Particles and Health: Lines that Divide. *J. Air Waste Manage. Assoc.* 47: 551–581.

Venkataraman, C. and Raymond, J. (1998). Estimating the Lung Deposition of Particulate Polycyclic Aromatic Hydrocarbons Associated with Multimodal Urban Aerosols. *Inhalation Toxicol.* 10: 183–204.

Wiedensohler, A. (1988). An Approximation of the Bipolar Charge Distribution for Particles in the Submicron Range. *J. Aerosol Sci.* 19: 387–389.

Zhu, C.S., Chen, C.C., Cao, J.J., Tsai, C.J., Chou, C.C.K., Liu, S.C. and Roam, G.D. (2010a). Characterization of Carbon Fractions for Atmospheric Fine Particles and Nanoparticles in a Highway Tunnel. *Atmos. Environ.* 44: 2668–2673.

Zhu, C.S., Cao, J.J., Tsai, C.J., Shen, Z.X., Ho, K.F. and Liu, S.X. (2010b). The Indoor and Outdoor Carbonaceous Pollution during Winter and Summer in Rural Areas of Shaanxi, China. *Aerosol Air Qual. Res.* 10: 550–558.

Received for review, October 6, 2010
Accepted, December 26 2010